

Electronic Supplementary Information

Photo-induced sol-gel processing for low-temperature fabrication of high performance silsesquioxane membranes for molecular separation

M. Nishibayashi,^a H. Yoshida,^a M. Uenishi,^b M. Kanezashi,^a H. Nagasawa,^a T. Yoshioka^a and T. Tsuru^{*a}

^a Department of Chemical Engineering, Hiroshima University, 1-4-1 Kagamiyama, Higashi-Hiroshima, 739-8527, Japan. E-mail: tsuru@hiroshima-u.ac.jp; Fax: +81 82 424 5494; Tel: +81 82 424 7714

^b Toyohashi Corporate Research Laboratories, Mitsubishi Rayon Co., Ltd., 4-1-2 Ushikawa-Dohri, Toyohashi 440-8601, Japan.

ESI-1:

Fig. S1 shows the UV-curing time course of FT-IR absorbance area of SiOH (900cm^{-1}) and SiOCH₃ groups (2980cm^{-1}) normalized with SiOSi groups ($1050\sim 1200\text{cm}^{-1}$). After 1min irradiation, SiOCH₃ groups almost completely decomposed, and SiOH groups also decreased, showing high reactivity of photo-induced reaction. This shows that photo-polymerization occurs in the short time, and has high reactivity

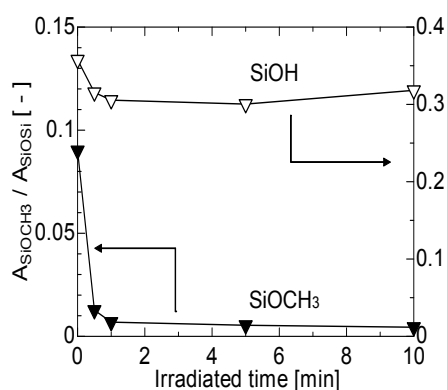


Fig. S1 Time course of SiOH and SiOCH₃ absorbance area ratio normalized with SiOSi.

ESI-2:

Fig. S2 shows the time course of pencil hardness, under UV irradiation, of BTMSE-derived films with/without Irgacure250 on the glass slides. After 1 min irradiation, the film with IRACURE250 was solidified with 2H hardness, while the films without Irgacure250 remained viscous liquid. This shows that photo-polymerization cured the films in the short time.

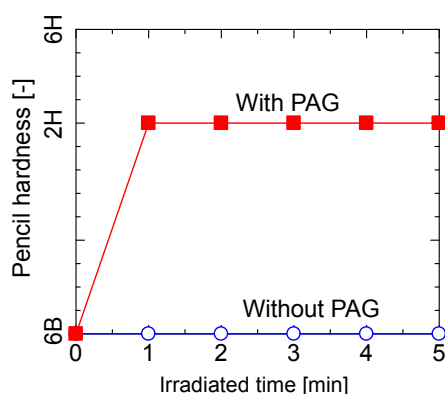


Fig. S2 Time course of pencil hardness of with/without PAG films.

ESI-3:

For evaluation of abrasion resistance, MAPTMS-derived sols mixed with radical and cationic photoinitiator were coated on acrylic plates and dried in N₂ and air 10 min, respectively. The results of abrasion resistance test of MAC-SQ films is shown in Fig. S3. The surface of acrylic plate without coating were scratched, while that with coating and UV-irradiation was difficult to scratch. UV-films were confirmed to be cured by UV-irradiation. After 10 min irradiation in air, cationic photo-polymerization films were more difficult to scratch than radical photo-polymerization films probably because radical photo-polymerization was inhibited by O₂, which might have remained in the reaction chamber.

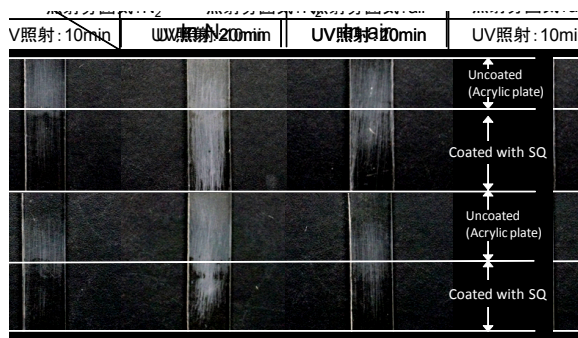


Fig. S3 Abrasion resistance test of MAC-SQ films (radical and cationic reaction, irradiated 10, 20 min)

ESI-4:

Fig. S4 shows the preparation of SiO₂ZrO₂ intermediate layers. 0.5wt% TiO₂-peptized sols were coated on the outer surface of a porous support (pore size: 150 nm, outer diameter 3 mm, length: 10cm), followed by firing at 550°C for 15 min in air. Then, SiO₂-ZrO₂ (Si/Zr=1/1) sol, which was prepared from tetraethoxysilane (TEOS) and zirconium tetrabutoxide (ZrTB) and diluted to 0.5wt%, was coated onto the substrate to form an intermediate layer with pore sizes of several nm. Then, the BTMSE-derived and MAPTMS-derived silica layer were fabricated by coating a BTMSE sols and MAPTMS sols, respectively. The pore size distribution was evaluated by Nanopermporometry using hexane as a condensable gas. The detailed nanoporometry can be found elsewhere (Tsuru et al., J. Membr. Sci., 186 (2001) 257-265.)

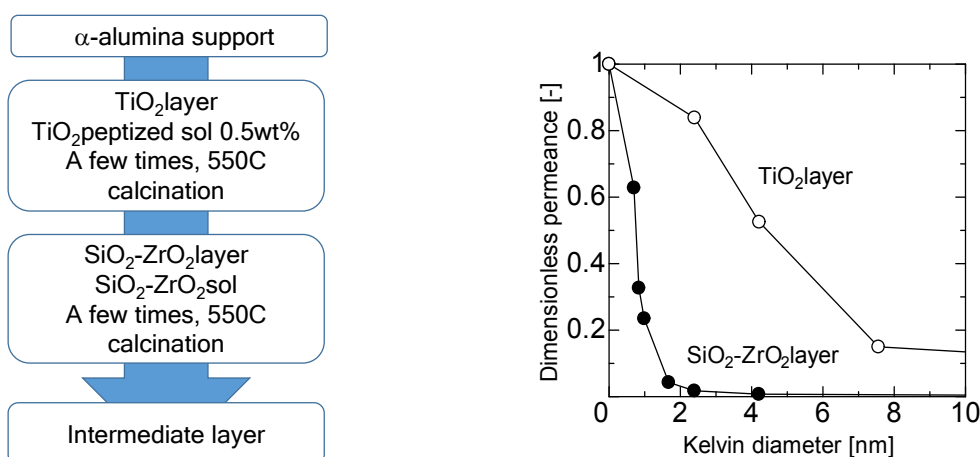


Fig. S4 Preparation of intermediate layer (left) and the pore size distribution (right).

ESI-5:

After coating BTMSE and MAPTMS sols on the intermediate layer, the substrate was set in the quartz cell, and irradiated UV for 12 min. For all-round irradiation of a cylindrical support, the substrate was rotated 90° every 3 min irradiation as shown in Fig. S5.

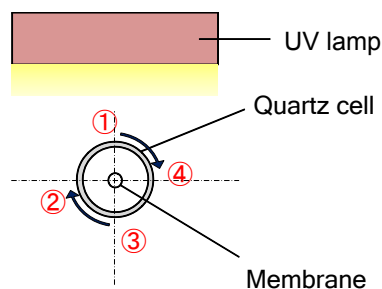


Fig. S5 Schematic representation of membrane rotation for UV-irradiation.

ESI-6:

BTMSE films were coated onto quartz plates (20 mm x 10 mm; thickness: 1 mm) in the same manner as silicon wafers, so that the thickness of the MBTMSE film was 100-200 nm, approximately the same thickness as that of the separation layer in BTMSE membranes (Fig. 5). Fig. S6 shows the UV/Vis spectra of BTMSE-derived films before and after UV irradiation for 5 min. The reference spectra were collected using an uncoated quartz plate. As shown in the figure, BTMSE-coated films showed an absorbance that was 200-300 nm less than 0.1, which indicates most of the UV (larger than 90%) penetrated the BTMSE layers that were 100-200 nm thick. Therefore, the BTMSE-derived layers coated onto porous supports (Fig. 5) were fully cured by UV irradiation. Interestingly, after UV irradiation, an absorption peak at 250 nm shifted to 260-280 nm, probably because the PAG (Irgacure 250) was partially decomposed.

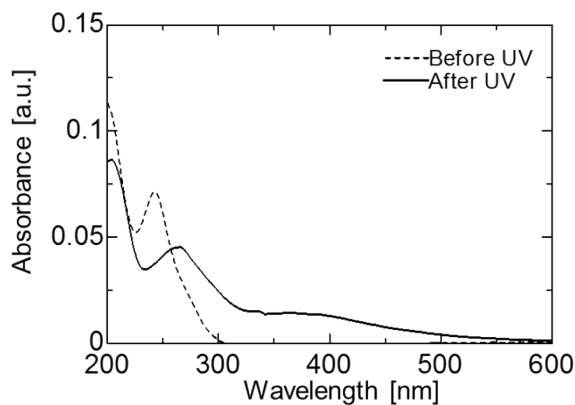


Fig. S6 UV/Vis spectra of BTMSE films (dotted and solid curves: before and after UV irradiation for 5 min.)

ESI-7

A schematic diagram of the apparatus used for pervaporation (PV) is shown in Fig. S7. For the pervaporation experiments, the membrane was dipped into the liquid feed mixture (upstream), the temperature of which was controlled with a heater. The inside of the cylindrical membrane was evaluated using a vacuum pump. The feed solution was vigorously circulated with an agitation screw to reduce the effects of concentration and temperature polarization. PV experiments of water/isopropanol (water: 10 wt%) were carried out at 40°C.

Permeance was calculated using $P_i = J_i / (p_{1i} - p_{2i})$ where J_i is the permeate mole flux, and p_{1i} and p_{2i} are the partial pressures for the feed and permeate stream, respectively. The partial pressures of the feed side was obtained using the Antoine equation for saturated vapor pressure and the Wilson equation for the activity coefficients, while the vapor

pressure in the permeate p_{2i} was assumed to be zero.

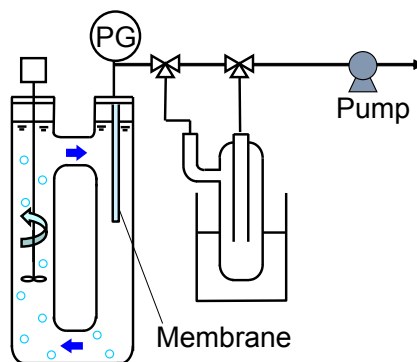


Fig. S7 Schematic figure of the PV apparatus.

ESI-8:

An initial increase in separation factor with a water permeance that was approximately unchanged was often observed in the pervaporation of organic aqueous solutions via not only SQ (bis(triethoxysilyl)ethane (BTESE)) membranes^{7,8} but also ceramic membranes such as $\text{SiO}_2\text{-ZrO}_2$.¹⁶ Both types of membranes showed a gradual decrease in IPA flux in the initial several hours and reached a steady state, while H_2O flux decreased only slightly.

We reported that this could be ascribed to the adsorption of IPA molecules on the hydrophilic portions of large pores, which allowed IPA permeation.^{7,8,16} The adsorbed IPA, which was confirmed by adsorption experiments,¹⁶ made the effective pore size small enough and consequently reduced the permeate flux of IPA. Regarding H_2O permeation, since most of the H_2O permeated through small pores, as reasonably suggested by the high separation factor, the adsorbed IPA did not affect the H_2O flux.

ESI-9:

The time courses of H_2O /IPA pervaporation characterization of MAPTMS-UV membrane prepared using with Irgacure250 were shown in Fig. S8. MAPTMS-UV membrane showed high separation factor of about 30, while that of $\text{SiO}_2\text{-ZrO}_2/\text{TiO}_2$ intermediate layer membrane was 1.95, which is close to gas-liquid equilibrium of 1.15.

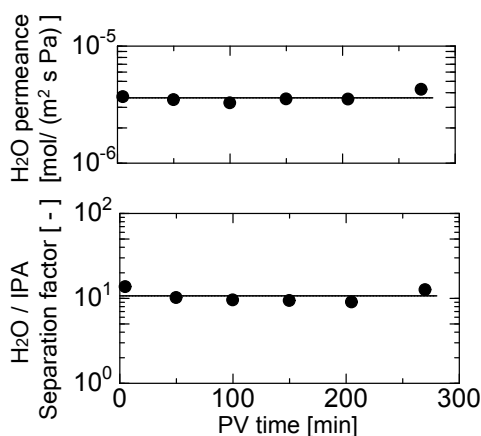


Fig. S8 Time course of separation factor and permeance of MAPTMS-UV membrane ($\text{H}_2\text{O}/\text{IPA}=1/9$).